Check for updates

Pharmacological enhancement of slow-wave activity at an early disease stage improves cognition and reduces amyloid pathology in a mouse model of Alzheimer's disease

Sedef Kollarik[1,2,3], Dorita Bimbiryte[1], Aakriti Sethi[1], Inês Dias[1,2,4], Carlos G. Moreira[1] and Daniela Noain[1,2,3,5]*

[1]Department of Neurology, University Hospital of Zurich, Zurich, Switzerland, [2]Neuroscience Centre Zurich (ZNZ), Zurich, Switzerland, [3]University of Zurich, Zurich, Switzerland, [4]D-HEST, ETH Zurich, Zurich, Switzerland, [5]University Center of Competence Sleep and Health Zurich, University of Zurich, Zurich, Switzerland

Introduction: Improving sleep in murine Alzheimer's disease (AD) is associated with reduced brain amyloidosis. However, the window of opportunity for successful sleep-targeted interventions, regarding the reduction in pathological hallmarks and related cognitive performance, remains poorly characterized.

Methods: Here, we enhanced slow-wave activity (SWA) during sleep via sodium oxybate (SO) oral administration for 2 weeks at early (6 months old) or moderately late (11 months old) disease stages in Tg2576 mice and evaluated resulting neuropathology and behavioral performance.

Results: We observed that the cognitive performance of 6-month-old Tg2576 mice significantly improved upon SO treatment, whereas no change was observed in 11-month-old mice. Histochemical assessment of amyloid plaques demonstrated that SO-treated 11-month-old Tg2576 mice had significantly less plaque burden than placebo-treated ones, whereas ELISA of insoluble protein fractions from brains of 6-month-old Tg2576 mice indicated lower Aβ-42/Aβ-40 ratio in SO-treated group vs. placebo-treated controls.

Discussion: Altogether, our results suggest that SWA-dependent reduction in brain amyloidosis leads to alleviated behavioral impairment in Tg2576 mice only if administered early in the disease course, potentially highlighting the key importance of early sleep-based interventions in clinical cohorts.

KEYWORDS

Alzheimer's disease, sleep, memory, mouse model, amyloidosis

1 Introduction

Sleep disturbances are believed to contribute to the development of neurodegenerative disorders such as Alzheimer's disease (AD), as they are highly prevalent in the preclinical stages (Ju et al., 2013), and linked to deterioration of disease symptoms. This association between AD and sleep renders the latter a promising target for potential treatment strategies to prevent or delay the onset of AD and/or to ameliorate the cognitive decline in AD patients (Ju et al., 2014).

Studies in both animals and humans have demonstrated that extracellular amyloid beta (Aβ) can accumulate in brain regions that regulate sleep/wake patterns, resulting in increased wakefulness (Braak and Braak, 1995; Roh et al., 2012). Evidence from a study measuring 24-h activity rhythms in over 300 participants revealed that higher fragmentation was associated with Aβ burden, particularly in ApoE4 carriers (Nguyen Ho et al., 2024). A community-based study also showed that high sleep fragmentation is associated with a higher risk of developing AD in a 6-year follow-up period (Lim et al., 2013). Moreover, subjective sleep impairments (Branger et al., 2016; Spira et al., 2018; Spira et al., 2013; Sprecher et al., 2015; Vicente De Carvalho et al., 2018) and disrupted sleep architecture, such as deficits in generating non-rapid-eye-movement sleep (NREM) slow-wave activity (SWA), a key restorative feature of deep sleep characterized by high-amplitude, low-frequency brain waves; Mander et al. (2015), are predictive of higher Aβ burden, as measured by positron emission tomography. Overall, these findings suggest a bidirectional relationship between Aβ levels and sleep regulation: while Aβ accumulation disrupts sleep, impaired sleep also worsens the disease progression, as observed in both animal models of AD (Kang et al., 2009; Park et al., 2023) and patients (Bianchetti et al., 1995; Ooms et al., 2014; Wennberg et al., 2017).

Sleep is intricately linked not only to amyloid burden but also to cognitive outcomes in AD and other dementias. The relationship between self-reported sleep (Kaprio and Koskenvuo, 2002) and 15–26 years post-survey cognitive outcomes in more than 2000 people ≥65 years old indicated that especially long-standing short sleep and poor sleep quality are deleterious for cognitive performance (Virta et al., 2013). In a cross-sectional study with asymptomatic AD patients, researchers observed that longer sleep duration was connected with lower Aβ load in regions of the brain characterized by early deposition (Aslanyan et al., 2023), suggesting strategies to improve sleep quality could potentially help delay the onset of cognitive symptoms associated with AD pathology. In fact, midlife sleep length and quality are associated with late-life cognitive function.

Abnormal expressions of circadian clock genes were observed in mice following chronic sleep deprivation, with these changes being more pronounced in AD mice than WT controls (Niu et al., 2022), indicating that sleep disturbances may have a greater impact on individuals with AD and emphasizing the need for targeted interventions to improve sleep as a potential strategy to mitigate AD progression.

In particular, studies suggest that sleep restoration may lead to improvements in several areas relevant to Alzheimer's symptoms. For instance, rescuing sleep alterations via chemogenetic manipulation of reticular nucleus activity in AD mice resulted in reduced accumulation of Aβ (Jagirdar et al., 2021), highlighting the putative importance of sleep-based neuroprotective interventions. Moreover, numerous studies showed that melatonin, a circadian rhythm–regulating hormone, plays a neuroprotective role against AD neuropathology (Hossain et al., 2019; Hossain et al., 2021; Lin et al., 2013).

Regarding mechanistic links between AD pathology and sleep, research has shown that release of Aβ is driven by neuronal hyperactivity (Bero et al., 2011; Cirrito et al., 2005; Nitsch et al., 1993) and concentration of Aβ in the brain parenchyma increases during wakefulness while decreasing during sleep (Kang et al., 2009; Musiek and Holtzman, 2016). In fact, not only the reduction in Aβ release but also the clearance of it from the interstitial space via the glymphatic

pathway appears to be facilitated by sleep, particularly associated with elevated SWA (Iliff et al., 2012; Mendelsohn and Larrick, 2013). Altogether, this evidence suggests that improving sleep quality may thus enhance the ability of the brain to reduce Aβ load, potentially offering a therapeutic strategy for mitigating Alzheimer's risk and/or slowing its progression.

Currently, there are no universally accepted effective treatments able to slow AD progression and relieve cognitive symptoms in patients (Livingston et al., 2024; Passeri et al., 2022). Sleep, contrasting to other prominent risk factors and/or outcomes of AD pathology, such as ApoE genotype, brain atrophy, or decreased cerebral blood flow, is a modifiable variable of relatively easy access. Thus, restoring sleep quality is a promising target to alleviate disease pathology and symptoms and modulating SWA during NREMS presents a valuable research opportunity with potential clinical application. However, there is a lack of interventional studies enhancing sleep during different progression stages of AD, which are crucial to determine whether sleep-based interventions may slow or stop disease progression. Here, aiming to determine the window of opportunity for sleep-based therapeutics to effectively ameliorate AD hallmarks, we investigate the effect of 2-week sodium oxybate (SO) oral administration on SWA electroencephalographic (EEG) measures, amyloid pathology, and behavioral performance in a mouse model of AD in two distinct disease stages: plaque free (early intervention) and plaque burdened (late intervention).
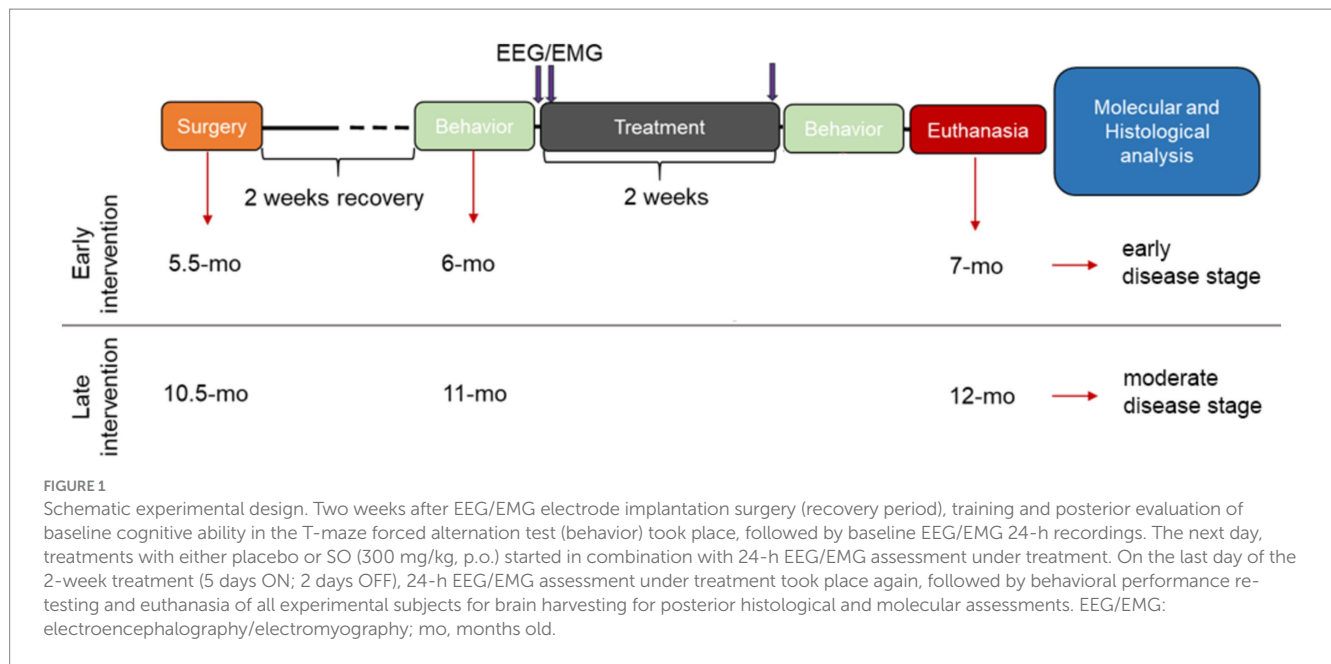
2 Materials and methods

2.1 Animals

We used male and female Tg2576 (Hsiao et al., 1996) mice (aged 6 months old for early intervention, and 11 months old for late intervention) overexpressing a mutant form of amyloid precursor protein (APP), APPK670/671 L, linked to early-onset familial AD, and non-transgenic WT mice from the same strain (Taconic Biosciences; Cologne, Germany). The animal room temperature was constant at 21–23°C, with a 12:12 h light:dark cycle (8 am/9 am ON, 8 pm/9 pm OFF, according to daylight saving time). Mice were housed in groups, had access to food and water *ad libitum,* and received daily routine health checks throughout the study. The study was conducted with the approval of the Cantonal Veterinary Office Zurich under license ZH210/17.

2.2 Experimental design

All mice underwent electroencephalography/electromyography (EEG/EMG) implantation surgery two weeks prior to the start of the intervention periods (early and late intervention, Figure 1). Subjects were randomly allocated to the placebo or the SO treatment group, within each genotype. Baseline (BL) cognitive ability and 24-h sleep/wake behavior were assessed before the treatment period started. SO (Xyrem®, UCB; 300 mg/kg, p.o.; SO half-life time = 20–40 min (Robinson and Keating, 2007)) and placebo (Xyrem®-placebo—no sodium oxybate in the formula, UCB; 300 mg/kg, p.o.) treatments were administered two times daily (ZT1 and ZT9) for 2 weeks [weekdays ON, weekends OFF regime (Kollarik et al., 2023; Morawska et al., 2021)]; 24-h sleep/wake recordings were re-evaluated during treatment, and cognitive ability was re-tested after the treatment period was concluded. Finally, the mice were

FIGURE 1
Schematic experimental design. Two weeks after EEG/EMG electrode implantation surgery (recovery period), training and posterior evaluation of baseline cognitive ability in the T-maze forced alternation test (behavior) took place, followed by baseline EEG/EMG 24-h recordings. The next day, treatments with either placebo or SO (300 mg/kg, p.o.) started in combination with 24-h EEG/EMG assessment under treatment. On the last day of the 2-week treatment (5 days ON; 2 days OFF), 24-h EEG/EMG assessment under treatment took place again, followed by behavioral performance re-testing and euthanasia of all experimental subjects for brain harvesting for posterior histological and molecular assessments. EEG/EMG: electroencephalography/electromyography; mo, months old.

euthanized via intraperitoneal injection of sodium pentobarbital followed by cervical dislocation, and their brains were harvested for further molecular and histological analyses.

2.3 EEG/EMG implantation surgery

We performed all surgical procedures under deep inhalation anesthesia with isoflurane (4–4.5% for induction in anesthesia box; 2–2.5% for maintenance using a nose cone fitting) and applied lidocaine, a local anesthetic (Xylocaine, Zurich) on the surface of the head skin prior to surgery. At the end of the surgery, we administered a combination of an anti-inflammatory (5 mg/kg, s.c., Metacam®, Zurich) and a pain relief drug (0.1 mg/kg, s.c., Temgesic®, Zurich), to further prevent postoperative inflammation and pain.

The animals were implanted as described before (Buchele et al., 2016). Briefly, we placed two stainless steel screws (Bossard, #BN650, 1,421,611), one for each hemisphere, located 2 mm posterior to Bregma, 2 mm lateral from midline. We then inserted two gold wires bilaterally into the neck muscles and applied sutures to close the skin around the implant. We connected the peridural screws and the muscle leads to a pin header (Farnell, #M80-8530445) for EEG and EMG recording, and fixed the structure with dental cement. Postsurgical analgesia was administered throughout the 3 days following the surgery during both light (0.1 mg/kg, s.c., Temgesic®, Zurich) and dark (1 mg/kg via drinking water, Temgesic®, Zurich) periods. We monitored wound healing, body weight, and home cage activity on a daily basis during the first week after the surgery and one time per week thereafter.

2.4 Data acquisition, EEG scoring, and post-processing

A 24-h EEG/EMG recording took place after a ~ 48-h habituation to recording conditions in all mice. The mice were tethered to a

rotating swivel and had access to every corner of the recording chamber. Signals were amplified using an N700 polysomnography (PSG) amplifier (Embla, Ontario, Canada) with a bipolar montage, digitized and collected at a sampling rate approximately 200 Hz and an input range of ±200 mV using a 16-bit digital-to-analog-converter. Data were collected via Somnologica Science, version 3.3.1 (ResMed, Saint-Priest, France). The scoring of the vigilance states was determined using SPINDLE (Miladinović et al., 2019). Post-processing of EEG signals was carried out using MATLAB (ver. R2019b) as described before (Kollarik et al., 2023). Briefly, we first removed artifacts by detecting clipping events, followed by a three-point moving average and a basic Fermi window function. Then, we resampled EEG signals at 200 Hz and filtered them between 0.5 and 30 Hz using low- and high-pass zero-phased equiripple FIR filters (Parks–McClellan algorithm; applied in both directions, filtfilt). We inspected the signal for regional artifacts not detected during automatic scoring or the above-mentioned preprocessing steps. Within scored NREMS, brief portions of the signal (<7 sample points at 200 Hz) > ± [8× interquartile range] were reconstructed by piecewise cubic spline interpolation from the neighboring points. Finally, we extracted measures of power in specific bandwidths, by performing a spectral analysis of consecutive 4-s epochs (FFT routine, Hamming window, 2-s overlap, and resolution of 0.25 Hz) and normalized the data indicating the percentage of each bin with reference to the total spectral power between 0.5 and 30 Hz.

2.5 Forced alternation T-maze test

We trained the mice in a forced alternation T-maze test adapted from a previous study (Deacon and Rawlins, 2006). First, we fed the mice with the reward in the home cages to habituate them to their taste and eliminate hyponeophagia. From the day prior to the test until the end of the test, all animals were restricted to eating 1.5 g/mouse/day of regular chow to increase the motivation for the reward. We split the 1.5 g of food into small pieces and recorded the weights of the mice

daily throughout the experiments in order to monitor and prevent potential monopolization of the food by the dominant mouse in the cage. On the second day, we habituated the mice to the enclosed maze by raising all doors, filling the food wells with rewards, and placing at once an entire home cage group in the maze for 3 min. After the habituation day, we trained each subject in three trials per day for 2 days, with an inter-trial interval of ca. 20 min for each mouse. Each trial consisted of two parts: the first one was a forced attempt, in which one of the arms was blocked by a door constraining the mouse to choose the open arm. The second part of the trial consisted of a choice attempt that started after the mouse consumed the reward in the open arm—or explored the arm for 2 min—and was placed back in the starting point facing away from the goal arms, and the forcing door was raised. Thus, in the second half of the trial, both goal arms were opened, but only the arm that had been previously blocked contained a food reward. Entering this previously unexplored, now rewarded arm was recorded as a "correct" response, while choosing the initially sole-available arm was recorded as an "incorrect" response. On the experimental day, each mouse was subjected to four trials. Testing timing before and after treatment was kept constant for each mouse, and all tests were conducted between ZT2 and ZT5.

2.6 Immunohistochemistry and stereology

After fresh harvesting, the brains were split into left and right hemi-brains. A randomly chosen hemi-brain was post-fixed in 4% paraformaldehyde in phosphate saline buffer (PBS), and the remaining hemi-brain was placed in a 1.5-ml Eppendorf tube and immediately snap frozen in liquid nitrogen. The post-fixed hemi-brains were dehydrated in sequential 15 and 30% sucrose in PBS solutions, then embedded in 30% sucrose molds, and then cut into 40-μm-thick sagittal sections using a freezing stage-equipped microtome (Leica SM2000 R). Every sixth section was selected and mounted onto gelatinized SuperFrost Ultra Plus slides and dried at 37°C overnight, amounting to a total of five sections per mouse.

2.6.1 4g8 staining

The mounted sections were washed in Tris–HCl buffered saline (TBS), incubated in 70% formic acid for 15 min, washed again in TBS, and incubated in 0.6% hydrogen peroxide (H_2O_2) for 30 min at room temperature to quench endogenous peroxidase activity. Then, sections were rinsed in TBS and blocked in M.O.M blocking reagent (Vector Laboratories, BMK-2202) diluted in 0.3% Triton-X in TBS (PH: 7.5–7.8) at room temperature for 1 h. After rinsing in TBS, the sections were first incubated for 10 min in a working solution of M.O.M Diluent at room temperature and then in primary antibody (1:2000, 4 g8 antibody, Covance, Cat. No. 800701, diluted in M.O.M Diluent) overnight at 4°C with gentle shaking. The following day they were incubated in M.O.M. Biotinylated Anti-Mouse IgG Reagent (Vector Laboratories) for 15 min and then in freshly prepared ABC elite solution for 1 h. After washing first in TBS and then with Tris-based buffered saline (TB) (pH = 7.6), the sections were developed in DAB (0.025%) and H_2O_2 (0.05%) in TBS for 25 min. The reaction was stopped by washing them three times for 10 min in TB. Subsequently, the slides were immersed in a series of ethanol solutions of increasing concentrations until 100%, then in a Xylene substitute (Roticlear®), and finally coverslipped with a mounting reagent (Rotimount®).

2.6.2 Congo red staining

Congo red staining was conducted as previously described for cerebral amyloid angiopathy (Wilcock et al., 2006). Briefly, the mounted sagittal brain sections were first rehydrated by immersing the slides in distilled water for 30 s. This was followed by a two-step incubation process: first, the sections were placed in an alkaline saturated NaCl for 20 min and then incubated in Congo red solution for 40 min. The slides were rinsed briefly in 95 and 100% ethanol solution and subsequently treated with three series of Xylene, each for 5 min. Finally, the slides were coverslipped with a mounting reagent.

2.6.3 Stereology

Five sagittal sections per mouse were used for stereological estimations. The area fraction fractionator probe (Stereoinvestigator™, MBF Bioscience) was used to estimate the areas covered by plaques in the regions of interest (ROI). The plaques were visualized with a Zeiss Imager M2 using a 20x objective, the size of the counting frame was 150×150 μm for the hippocampus and 200×200 μm for the cortex. The random sampling grid size was identical to the counting frame size in order to scan the entire ROI.

2.7 Brain homogenization and ELISA

We mechanically homogenized the frozen hemi-brains and sequentially extracted soluble and insoluble proteins with diethylamine (DEA) and formic acid (FA), respectively (Casali and Landreth, 2016). Aβ content in soluble and insoluble brain extracts was assessed by sandwich ELISA as indicated by the manufacturer of the kit (Aβ-40: KMB3481, Aβ-42: KMB3441, Thermo Fisher). To serve as controls, the placebo-treated Tg2576 brains were blindly processed in an identical fashion and in parallel to SO-treated Tg2576 brains throughout the entire process. Soluble and insoluble Aβ-40 and Aβ-42 were normalized to brain tissue mass and expressed in picogram per milligram.

2.8 Statistical analyses

Data analyses were carried out using IBM® SPSS® Statistics 25 software, and the data were visualized by GraphPad Prism 9 (GraphPad Software, Inc., San Diego, CA). Outliers were detected with boxplots, normality was assessed using skewness and kurtosis for each variable, and homogeneity of variances was assessed with Levene's test. Delta activity gain was analyzed with multiple t-tests for each hour, and p-values were corrected with the false discovery method in GraphPad Prism 9. NREMS proportion was analyzed with two-way ANOVA (genotype*treatment). Analyses of the main effect of genotype and treatment were separately run and followed by pairwise comparisons. All pairwise comparisons were reported with 95% confidence intervals (CI) and p-values. The cognitive performance of the mice was assessed in two steps. First, we conducted independent t-tests to investigate the baseline differences between genotypes in each age group, separately. Second, we ran a paired t-test to evaluate the change in cognitive performance from baseline to after treatment in Tg2576 mice. Biserial correlation analysis was used to assess the relationship between delta activity gain and cognitive performance in Tg2576 mice after cognitive performance was

assigned to two categories: fail (≤ 50) or success (> 50). Briefly, we first computed point-biserial correlation in SPSS and then transformed the point-biserial correlation coefficient (r_{pb}) into the biserial correlation coefficient (r_b) as it has been described before (Field, 2012). The difference in levels of soluble and insoluble Aβ-40 and Aβ-42 between placebo- and SO-treated Tg2576 mice was assessed with an independent t-test. The plaque burden in the hippocampus and cortex was calculated by dividing the total area covered with plaques by the total area of ROI. Then, the data were analyzed with a two-way ANOVA (genotype*treatment), followed by analyses of the main effects of genotype and treatment, separately. Subsequently, pairwise analyses were run to assess whether there was a difference in plaque burden between placebo- and SO-treated mice within the same genotype and whether there was a difference between Tg2576 and WT mice within the same treatment. Pearson's correlation analysis was run to evaluate the relationship between delta power gain and plaque burden in the hippocampus. Quantitative estimates of amyloid plaque burden in WT and Tg2576 young and aged mice identified through Congo red staining were analyzed using independent-samples t-test.

3 Results

3.1 SO administration elicited delta activity gain with unaltered time spent in NREMS

Decreased delta power during sleep is associated with AD (Lee et al., 2020) and may be one of the factors that worsen disease symptoms (Bianchetti et al., 1995; Wennberg et al., 2017). Considering that Tg2576 mice present with reduced delta activity in NREMS (Kollarik et al., 2023), we first aimed to rescue the impaired delta activity by SO pharmacotherapy. We administered placebo or SO (300 mg/kg, p.o.) at ZT1 and ZT9 during the light period for all groups. As the first step, we evaluated whether such a pharmacological regime exerted an increase in the time spent in NREMS compared to the baseline. Our results demonstrate that administration of SO (300 mg/kg, p.o.) did not significantly alter the time spent in NREMS in any of the groups in comparison with their own baseline (Figures 2A,B). Delta activity gain, i.e., increased SWA, from baseline was especially observed after the administration of ZT9 in all groups treated with SO when compared with the placebo-treated groups (Figures 2C–F). A difference in delta activity gain between SO and placebo after the first hour of administration was apparent only in Tg2576 mice in the late intervention cohort (Figure 2F).

3.2 SO treatment improves cognitive performance in mice at an early stage of AD

Studies showed that memory loss starts at approximately 6 months of age in Tg2576 mice, which coincides with the appearance of detergent-insoluble Aβ aggregates (Westerman et al., 2002). Therefore, we first assessed the cognitive performance of Tg2576 mice and WT controls in the T-maze forced alternation test in both age groups, separately, to determine the existence of treatment-naïve (baseline, BL) differences in memory (Figures 3A,B). We observed that Tg2576 mice in both age groups (early intervention: $n = 17$, $M = 42.65$,

SD = 14.99; late intervention: $n = 20$, $M = 53.75$, SD = 29.43) performed poorly [early intervention: $t(26.21) = 4.884$, $p < 0.001$, Cohen's $d = 1.64$; late intervention: $t(36) = 2.753$, $p = 0.009$, Cohen's $d = 0.91$] compared to age-matched WT controls (early intervention: $n = 18$, $M = 79.63$, SD = 28.18; late intervention: $n = 18$, $M = 75.93$, SD = 18.28) in the T-maze test.
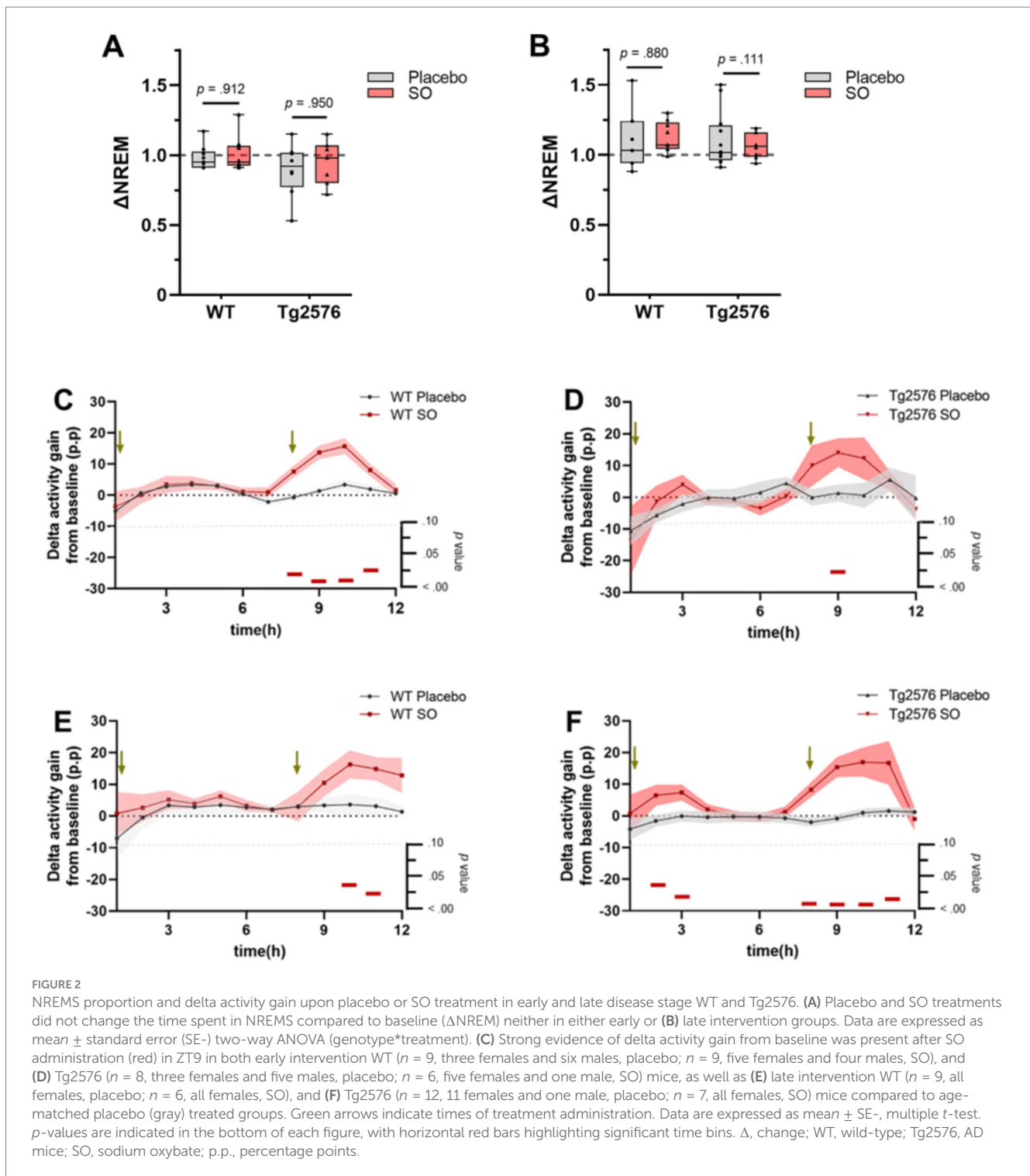
On the other hand, increases in high-amplitude SWA during NREMS may be associated with improved cognition (Wilckens et al., 2016). Thus, we analyzed cognitive performance of Tg2576 mice in both age groups after treatment (AT) with placebo or SO (Figures 3C,D). Our analyses revealed that cognitive performance in the early intervention SO group improved AT (Figure 3C) [BL: $M = 48.81$, SD = 18.90; AT: $M = 70.24$, SD = 9.45; $t(6) = 3.286$, $p = 0.017$, Cohen's $d = 1.43$], while treatments with placebo did not affect this outcome [BL: $M = 38.33$, SD = 10.54; AT: $M = 42.50$, SD = 28.18; $t(9) = 0.460$, $p = 0.657$, Cohen's $d = 0.20$]. There were no significant effects of either placebo [BL: $M = 52.50$, SD = 28.61; AT: $M = 46.67$, SD = 27.27; $t(9) = -0.771$, $p = 0.460$, Cohen's $d = 0.16$] or SO [BL: $M = 55.00$, SD = 31.72; AT: $M = 63.33$, SD = 31.23; $t(9) = 0.905$, $p = 0.389$, Cohen's $d = 0.26$] over Tg2576 mice cognitive ability in the late intervention group (Figure 3D).

3.3 Cognitive performance is positively correlated with SO-triggered delta activity gain

After determining increased delta activity and improved cognitive performance in Tg2576 mice after 2 weeks of oral SO administration, we examined whether there is an association between both measures. To this end, we first assigned the cognitive performance scores as fails ($\leq 50\%$) or successes ($> 50\%$) and then ran a biserial correlation between treatment-elicited delta activity gain after the second administration (delta gain in the 9th + 10th hours) in both treatments groups, i.e., placebo and SO, and cognitive performance in Tg2576 mice of both age groups, separately. Our analyses showed a trend toward a positive correlation between delta activity gain and cognitive performance in the early intervention group [$n = 8$, $r_{pb}(6) = 0.653$, $r_b = 0.819$, $p = 0.079$, Figure 4A], while there was no apparent correlation in the late intervention group [$n = 9$, $r_{pb}(7) = 0.563$, $r_b = 0.786$, $p = 0.114$, Figure 4B].

3.4 Histopathological evaluation of the baseline conditions in early and late intervention groups

Despite the progressiveness of AD pathology in Tg2576 mice has been widely reported before (Kawarabayashi et al., 2001), differences in the time onset suggested across individual colonies may lead to uncertain baseline conditions for longitudinal histopathological assessments. To determine the exact pathological stage in terms of plaque formation in the 6- and 11-month-old Tg2576 mice used in our study, as the basis for additional assessments of the effect of our treatment on pathology, we performed Congo red staining of sagittal brain sections from non-treated WT and Tg2576 mice across both age groups and quantitatively assessed plaque burden in the

FIGURE 2
NREMS proportion and delta activity gain upon placebo or SO treatment in early and late disease stage WT and Tg2576. **(A)** Placebo and SO treatments did not change the time spent in NREMS compared to baseline (ΔNREM) neither in either early or **(B)** late intervention groups. Data are expressed as mean $\pm$ standard error (SE-) two-way ANOVA (genotype*treatment). **(C)** Strong evidence of delta activity gain from baseline was present after SO administration (red) in ZT9 in both early intervention WT ($n = 9$, three females and six males, placebo; $n = 9$, five females and four males, SO), and **(D)** Tg2576 ($n = 8$, three females and five males, placebo; $n = 6$, five females and one male, SO) mice, as well as **(E)** late intervention WT ($n = 9$, all females, placebo; $n = 6$, all females, SO), and **(F)** Tg2576 ($n = 12$, 11 females and one male, placebo; $n = 7$, all females, SO) mice compared to age-matched placebo (gray) treated groups. Green arrows indicate times of treatment administration. Data are expressed as mean $\pm$ SE-, multiple t-test. p-values are indicated in the bottom of each figure, with horizontal red bars highlighting significant time bins. Δ, change; WT, wild-type; Tg2576, AD mice; SO, sodium oxybate; p.p., percentage points.

hippocampus (Figure 5). Representative photomicrographs from 11-month-old Tg2576 mice (Figures 5A–E) demonstrated a high level of plaque deposition in hippocampal areas. Stereological analyses confirmed a very low and indifferent plaque burden in WT and Tg2576 mice at the early disease stage [$t(6) = 0.169$, $p = 0.871$, Cohen's $d = 0.12$, Figure 5F], while evidencing a higher plaque burden in Tg2576 at moderately advanced disease stage [$t(7) = -3.850$, $p = 0.006$, Cohen's $d = 2.50$, Figure 5G] than age-matched WT littermates.

3.5 SO treatment results in reduced levels of toxic insoluble Aβ42/40 ratio and diminished plaque burden in early- and late-stage Tg2576 mice

Based on the quantification results of the Congo red staining showing now discernible plaque load in the Tg2576 mice at 6 months of age, agreeing with previous literature (Kawarabayashi et al., 2001), we proceeded to evaluate the effect of SO and placebo treatments onto
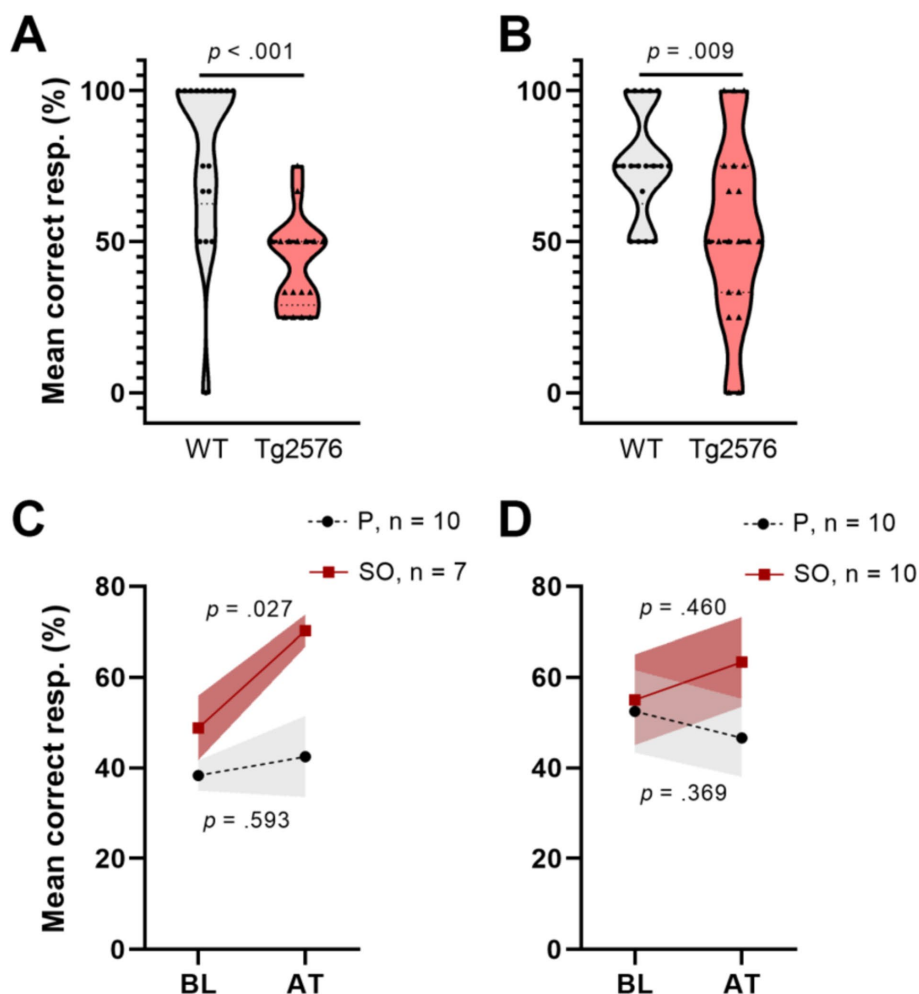
FIGURE 3
T-maze forced alternation test performance of early and moderate disease stage Tg2576 mice at baseline and upon treatment. **(A)** Tg2576 mice performed poorly in both early and **(B)** moderate disease stage in comparison with age-matched WT mice (independent *t*-test; early: *p* < 0.001; late: *p* = 0.009). **(C)** Early disease stage Tg2576 mice significantly improved performance values after 2 weeks of treatment with SO (*n* = 10, seven females and three males; paired *t*-test, *p* = 0.027), whereas placebo-treated mutants draw no benefit from the intervention (*n* = 7, two females and five males; paired *t*-test, *p* = 0.593). **(D)** Moderate disease stage Tg2576 mice do not present significantly improved performance scores upon treatment (*n* = 10, all females; paired *t*-test, *p* = 0.46), same as their placebo-treated counterparts (*n* = 10, all females; paired *t*-test, *p* = 0.369). Data are expressed as mea*n* ± SE-. resp., responses; WT, wild-type; Tg2576, AD mice; P, placebo; SO, sodium oxybate.

amyloidosis in this premorbid (plaque free) stage via determinations of soluble and insoluble Aβ-40 and Aβ-42 levels in brain tissue from Tg2576 mice via ELISA. We observed that soluble Aβ-40 [$t(8) = 0.638$, $p = 0.791$, Cohen's $d = 0.18$] and Aβ-42 [$t(8) = 0.280$, $p = 0.864$, Cohen's $d = 0.11$, Figures 6A,B] did not differ between treatments. Insoluble Aβ-40 level, on the other hand, was higher [$t(8) = 2.846$, $p = 0.022$, Cohen's $d = 1.80$] in the brains of SO-treated Tg2576 mice ($n = 5$, $M = 4.982$, SD = 0.379) in comparison with what was observed in the brains of placebo-treated Tg2576 mice ($n = 5$, $M = 4.459$, SD = 0.158, Figure 6D). Insoluble Aβ-42 levels did not differ [$t(8) = 0.597$, $p = 0.567$, Cohen's $d = 0.38$, Figure 6E] between treatments. Aβ-42/Aβ-40 ratio is considered a more accurate way of reflecting the progress of AD (Wiltfang et al., 2007) than Aβ-40 and Aβ-42 expressed separately. Therefore, we followed our analyses with the assessment of treatment-dependent changes in Aβ-42/Aβ-40 ratio. We did not detect a difference in the soluble Aβ-42/Aβ-40 ratio between treatments [$t(8) = 0.695$, $p = 0.723$, Cohen's $d = 0.23$,

Figure 6C], while our results indicated a trend with a large effect size toward a lower insoluble Aβ-42/Aβ-40 ratio in the brains of SO-treated Tg2576 mice [$t(8) = 2.009$, $p = 0.079$, Cohen's $d = 1.27$, Figure 6F] compared to placebo-treated controls.

Tg2576 mice have been reported to develop Aβ plaques as they age (Benzing et al., 1999; Hsiao et al., 1996; Ishii et al., 2014; Kawarabayashi et al., 2001), as confirmed by the significant difference in the load of Congo red-stained plaques between WT and Tg2576 mice at 11 months of age. In fact, the hippocampus and cortex are two primary regions vulnerable to plaque accumulation in AD (Bero et al., 2011). Therefore, we investigated plaque burden in both these key areas in brains from the late intervention cohort treated with placebo or SO. We included WT mice in our analyses as negative controls. We found strong evidence of reduced plaque burden in the hippocampal (Figures 7A–C) and cortical (Figures 7D–F) brain areas of Tg2576 mice after 2 weeks of treatment with SO. The interaction effect between genotype and treatment on plaque burden in the
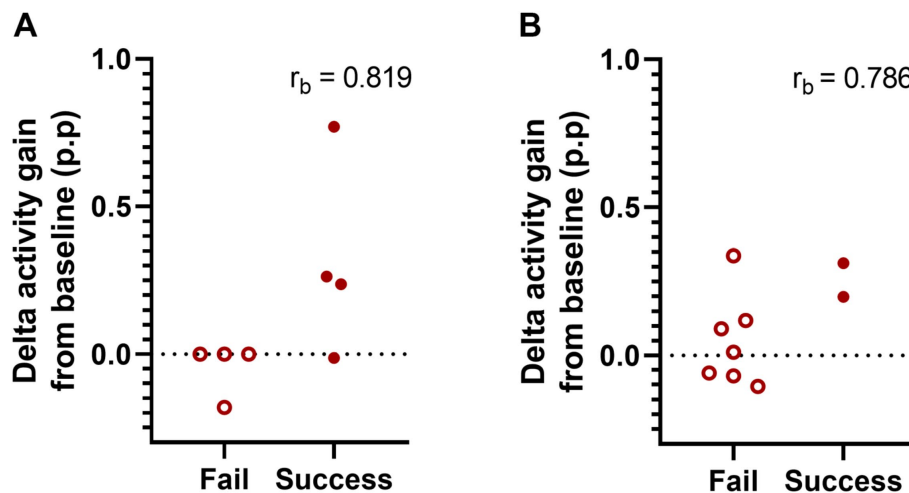
FIGURE 4
Association between delta activity gain and cognitive performance in early and moderate disease stage Tg2576 mice. **(A)** Biserial correlation analyses revealed a positive large correlation coefficient between delta activity gain and the cognitive performance in both early (n = 8, four females and four males) and **(B)** late intervention (n = 9, all females) cohorts. No significant results were identified due to small sample size. $0.1 < |r_b| < 0.3$ = small correlation, $0.3 < |r_b| < 0.5$ = medium/moderate correlation, $|r_b| > 0.5$ = large/strong correlation. p.p., percentage points.

hippocampus (Figure 7C) was a trend with a large effect size [$F(1, 28)$ = 3.807, p = 0.061, η_p^2 = 0.120]. The main effect of genotype on plaque burden was significant [$F(1, 28)$ = 10.820, p = 0.003, η_p^2 = 0.279], while the main effect of treatment was a trend [$F(1, 28)$ = 3.634, p = 0.067, η_p^2 = 0.115]. Following pairwise comparisons within the genotype, we observed a significant decrease in plaque burden in SO-treated Tg2576 mice, while there was no change in the placebo treatment group. There was no effect of treatment on the naturally low plaque burden in the hippocampus of WT mice. In particular, after 2 weeks of SO treatment, plaque burden in the hippocampus of Tg2576 mice was at a similar level to the plaque burden in WT mice. In the cortex, plaque burden analyses revealed similar results to those in the hippocampus (Figure 7F). The interaction effect between genotype and treatment on plaque burden in the cortex was a trend with a large effect size [$F(1, 28)$ = 4.054, p = 0.054, η_p^2 = 0.126]. There was a significant main effect of genotype [$F(1, 28)$ = 13.965, p = 0.001, η_p^2 = 0.333] but not of treatment [$F(1, 28)$ = 2.951, p = 0.097, η_p^2 = 0.095] on plaque burden. We followed the analyses with pairwise comparisons and observed a greater plaque burden in placebo-treated Tg2576 mice in comparison with SO-treated mutants. Within the placebo-treated mice, Tg2576 mice showed a higher plaque burden in the cortex than WT, while SO-treated mice did not differ between genotypes.

3.6 Reduction in plaque burden is associated with SO-triggered delta activity gain

Our findings of increased delta activity gain and decreased plaque burden in Tg2576 mice after treating with SO led us to investigate the relationship between both parameters. Therefore, we ran a Pearson's correlation between the plaque burden in the hippocampus and cortex (Figure 8), and delta activity gain after the second administration of the treatment (delta activity gain in the 9th + 10th hours). Our findings

demonstrated that mice that had higher delta activity gain showed less plaque burden in the hippocampus (r = −0.882, p = 0.020; Figure 8A), while no association was found between cortical plaque burden and delta activity gain (r = −0.065, p = 0.902; Figure 8B).

4 Discussion

Reduced sleep quality and duration are commonly observed phenomena associated with aging. Apart from being highly prevalent in the elderly population (Mander et al., 2017), sleep disturbances are often more severe and exacerbate disease symptoms in AD and other neurodegenerative diseases. Cumulating evidence supports a reciprocal relationship between sleep and AD, meaning that disturbed sleep is not only an outcome of AD but can also affect cognitive function and disease pathology in patients (Lucey et al., 2021; Wang and Holtzman, 2020). Drawing on this relationship, treatments targeting the restoration of sleep could be a promising approach to alleviating disease symptoms.

It was previously shown that enhancing sleep with a dual orexin antagonist decreased Aβ aggregation in a mouse model of AD (Kang et al., 2009). Moreover, another sleep-promoting neuromodulator, melatonin, inhibited the generation and formation of amyloid fibrils *in vitro* (Lin et al., 2013) and diminished tau hyperphosphorylation (Lin et al., 2013; Ling et al., 2009). In a previous study, we demonstrated that SWA enhancement via SO upregulates multiple proteostatic pathways with the capacity to regulate intra- and extracellular noxious protein levels in Parkinson's disease mice (Morawska et al., 2021). Moreover, optogenetic targeting of GABAergic interneurons in a mouse model of AD not only rescued sleep disruptions and sleep fragmentation by improving NREMS, delta power, and SWA but also increased microglial clearance ability resulting in phagocytic uptake of Aβ (Zhao et al., 2023). In the present study, as an SWA modulator we used SO, which is a GABA$_B$/GHB receptor agonist known to generate deep sleep-like increases in delta
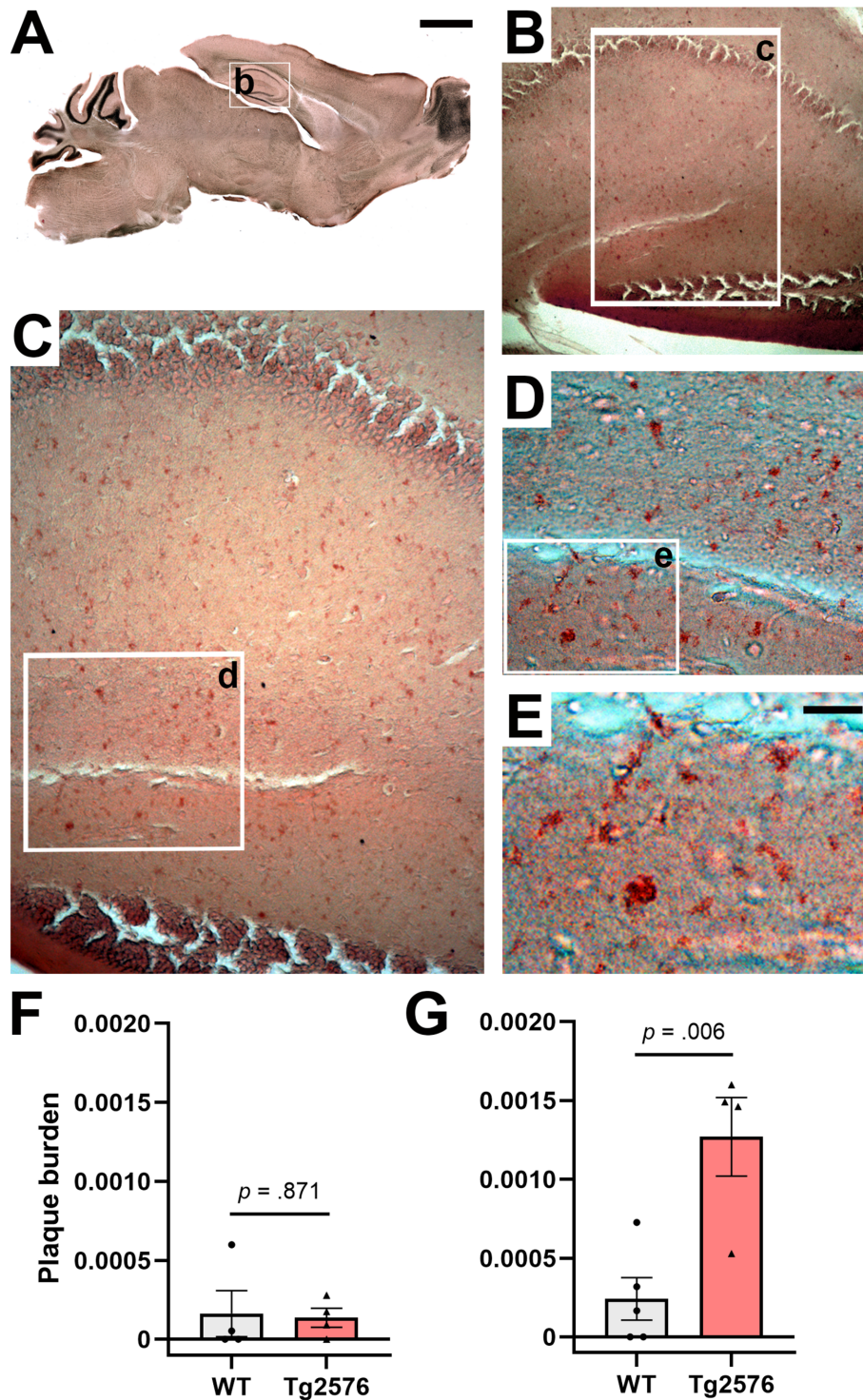
FIGURE 5
Congo red staining of hippocampal amyloid plaques in drug-naïve early and moderate disease stage WT and Tg2576 mice. **(A–E)** Representative photomicrographs illustrating Congo red positive deposits in hippocampal tissue of moderate disease stage Tg2576 mice. **(F)** Early disease stage Tg2576 mice ($n = 4$, two females and two males) and age-matched WT controls ($n = 4$, three females and one male) present low and indistinct levels of plaque burden in the hippocampus (independent t-test; $p = 0.871$), whereas **(G)** moderate disease stage Tg2576 mice ($n = 4$, all females) have a significantly higher plaque burden score than their age-matched WT controls ($n = 5$, all females; independent t-test; $p = 0.006$). WT, wild-type; Tg2576, AD mice. Scale bars: A = 2 mm, E = 50 μm.

power to investigate the restorative effect of SO-induced "deep sleep" on cognition and amyloidosis in a well-established mouse model of AD, the Tg2576 line.

AD pathogenesis in humans begins 10–20 years prior to the onset of clinical symptoms (Sperling et al., 2011). Thus, it is important to establish potential disease-modifying therapies targeting the
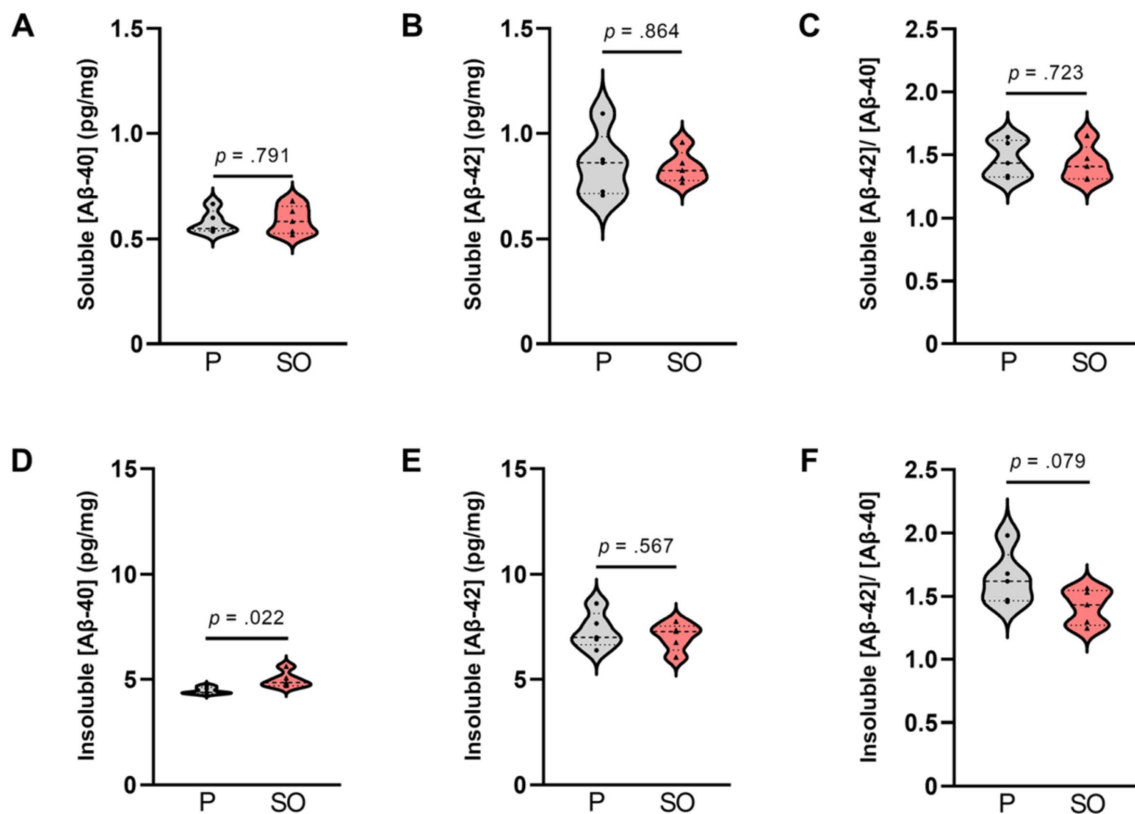
FIGURE 6
Soluble and insoluble Aβ-40 and Aβ-42 brain concentration upon treatments in early disease stage Tg2576 mice. **(A)** No differences in soluble [Aβ-40], **(B)** [Aβ-42], and **(C)** [Aβ-42/Aβ-40] ratio between placebo- and SO-treated brains of early disease stage Tg2576 mice (independent t-test; Aβ-40: $p = 0.791$, Aβ-42: $p = 0.864$; Aβ-42/Aβ-40: $p = 0.723$). **(D)** Insoluble [Aβ-40] was higher in the brains of SO-treated early disease stage Tg2576 mice in comparison with placebo-treated mutants (independent t-test; $p = 0.022$), whereas **(E)** insoluble [Aβ-42] did not differ between treatments (independent t-test; $p = 0.567$). **(F)** The ratio of insoluble [Aβ-42/Aβ-40] in brains of SO-treated early disease stage Tg2576 mice was slightly lower than that of placebo, with a trend statistical significance (independent t-test; $p = 0.079$). Data are expressed as mean $\pm$ SE-. [Aβ-40]: amyloid beta 40 concentration; [Aβ-42]: amyloid beta 42 concentration; P: placebo; SO, sodium oxybate ($n = 5$ per group, all females).

preclinical phase for the prevention of AD. It has been predicted that as small as a 1-year delay of AD symptoms onset can result in 11.8 million fewer cases worldwide, massively reducing the global burden of the disease (Brookmeyer et al., 2007). Moreover, the unsuccessful clinical translation of positive results obtained from targeting the late phases of AD in animal models (Knopman et al., 2019; Tampi et al., 2021) calls for novel therapeutic strategies focusing on prevention and/or delaying the onset of AD before the full spectrum of clinical hallmarks is present. In line with this, we designed our study to find an effective time course to start sleep-based treatments to potentially alleviate pathological features and cognitive symptoms of AD. Thus, we selected two relatively early age and treatment time points, in which mice are either in the pre-morbid stage (amyloid plaque-free) or moderate stage (amyloid plaque-burdened), which we successfully confirmed via quantitative analysis of Congo red staining.

Our findings indicate that oral SO administration with a dose of 300 mg/kg increases delta activity without changing the 24-h sleep amount in both Tg2576 and WT mice and provides evidence of reduced plaque deposition in both hippocampus and cortex in moderate disease stage Tg2576 mice. Consistent with our observations, Klein et al. showed decreased levels of Aβ due to enhanced activity of neprilysin after oral treatments with SO (Klein et al., 2015). Therefore, our study further contributes to existing

knowledge of the positive effect of "deep sleep" promotion on Aβ plaque clearance (Kang et al., 2009; Klein et al., 2015). Additionally, our correlation analysis revealed that the mice with higher delta activity gain after SO administration also presented lower plaque burden in the hippocampus; however, this correlation was not observed in the cortex. Future studies should consider subdividing the measurements into distinct cortical regions (e.g., prefrontal cortex, parietal cortex, and piriform cortex) to avoid data dilution.

Given the absence of stainable/visible plaques in Tg2576 mice at the age of 6–7 months (even incipient plaques are seen only at 11–12 months), we assessed amyloidosis via ELISA by investigating the levels of soluble and insoluble Aβ-40 and Aβ-42 and their respective ratios. Soluble Aβ levels showed no difference between placebo and SO-treated AD mice, potentially due to a 3-day drug washout period before euthanasia, allowing neuronal activity to normalize pathological soluble Aβ levels. Insoluble Aβ levels, on the other hand, revealed a significantly higher Aβ-40 level in SO-treated Tg2576 mice compared to placebo-treated ones, while insoluble Aβ-42 levels did not differ between treatments. Relatively higher levels of shorter, less fibrillogenic Aβ-40 in SO-treated mice emerge as an intriguing factor with potential neuroprotective implications, also previously discussed by others (Kim et al., 2007; Zoltowska et al., 2016). The slight
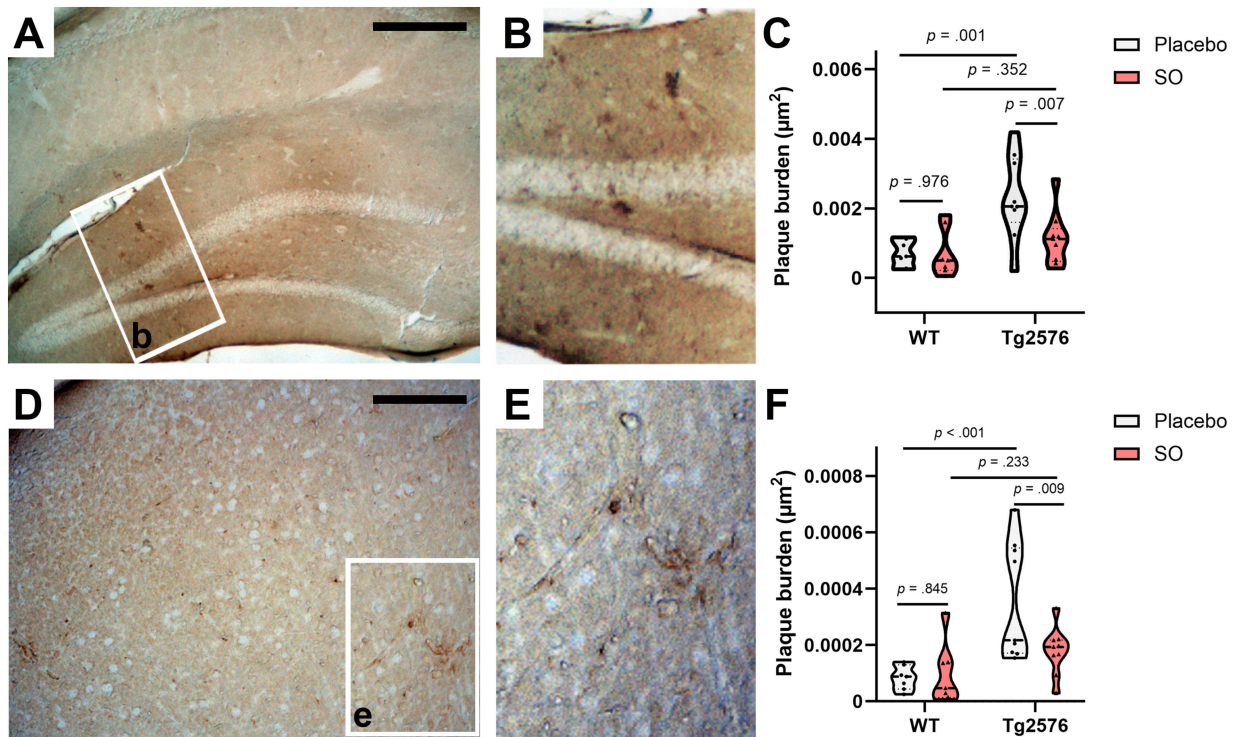
FIGURE 7
Hippocampal and cortical amyloid plaque burden upon treatments in moderate disease stage Tg2576 mice. **(A,B)** Representative photomicrographs of 4 g8-positive deposits in the brains of hippocampus of moderate disease stage Tg2576 mice. **(C)** Stereological estimates of plaque burden (µm²) in placebo-treated WT (*n* = 7, all females), SO-treated WT (*n* = 7, all females), placebo-treated Tg2576 (*n* = 9, all females), and brains of SO-treated Tg2576 (*n* = 9, eight females and one male) mice stained against Aβ (17−24) with 4 g8 antibody. A significant decrease in plaque burden was observed in the hippocampus of Tg2576 brains after 2-week treatment with SO compared to placebo-treated mutants (two-way ANOVA; pairwise comparisons, *p* = 0.007). **(D,E)** Representative photomicrographs of 4 g8-positive deposits in the cortex of the brains of moderate disease stage Tg2576 mice. **(F)** Stereological estimates of plaque burden (µm²) in brains of placebo-treated WT (*n* = 7), SO-treated WT (*n* = 7), placebo-treated Tg2576 (*n* = 9), and SO-treated Tg2576 (*n* = 9) mice stained against Aβ (17−24) with 4 g8 antibody. A significant decrease of plaque burden was observed in cortical regions of Tg2576 brains after two-week treatment with SO compared to placebo-treated mutants (two-way ANOVA; pairwise comparison, *p* = 0.009). All data are expressed as mean± SE-. WT, wild-type; Tg2576: AD mice; SO, sodium oxybate. Scale bars: A = 500 µm and D = 350 µm.
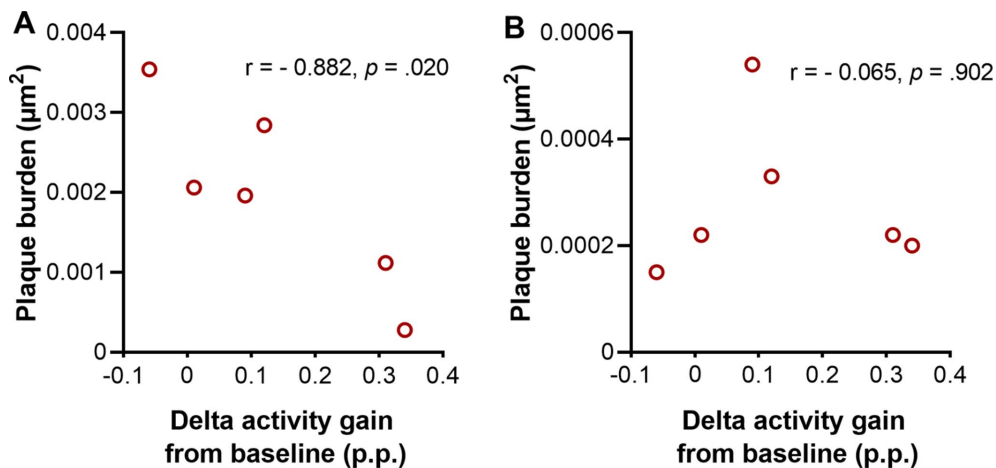

FIGURE 8
Association between delta activity gain and plaque burden in moderate disease stage Tg2576 mice. **(A)** Strong negative association between plaque burden in hippocampus and delta activity gain in moderate disease stage Tg2576 mice (Pearson's correlation coefficient *r* = −0.882, *p* = 0.020). **(B)** No association between plaque burden in cortex and delta activity gain was observed in the same mice (Pearson's correlation coefficient *r* = −0.065, *p* = 0.902). $0.1 < |r| < 0.3$ = small correlation, $0.3 < |r| < 0.5$ = medium/moderate correlation, $|r| > 0.5$ = large/strong correlation. p.p., percentage points (*n* = 6, all females).

reduction with a large effect size found in the Aβ-42/Aβ-40 ratio after 2 weeks of treatment with SO in early disease-stage mice may additionally suggest prevention neurotoxicity (Zoltowska et al., 2016).

Correlation analyses between delta activity gain and cognitive performance in Tg2576 mice, although observed in the expected direction with strong effect sizes, were not statistically significant for either age group. Therefore, future studies shall consider larger sample sizes to strengthen, particularly the behavioral analysis, as well as >1 day EEG/EMG recording for a better interpretation of these results.

Others have shown before that oral administration of SO via drinking water decreased levels of brain Aβ and reduced cognitive deficits in APPSWE mice (Klein et al., 2015). A limitation of that study, however, was the difficulty in controlling the dose of SO consumed by the animals, hindering the possibility of drawing links between specific sleep alterations elicited by the treatment and the observed effects. In fact, the study did not incorporate objective sleep measures, and as a result, a direct link between SO administration and its primary effect (i.e., enhanced SWA) could not be established. Thus, to the best of our knowledge, this is the first study reporting a differential effect of increased SWA on both amyloid pathology and cognitive symptoms in a disease-stage-dependent manner in a mouse model of AD.

Several limitations of our study, however, need to be taken into consideration. First, the absence of a model of tauopathy, another pathological hallmark of AD, which is strongly correlated with the disease symptoms, impairs our ability to generalize our findings to AD. Evaluating the efficacy of SO treatment on an appropriate model of tau pathology would be important for future studies. Second, we did not evaluate whether a longer period of treatment would be effective on the cognitive performance of Tg2576 in the moderate disease stage group. Knowing whether a longer duration of sleep treatment interventions may additionally help arrest symptoms at an advanced disease stage would be of great importance to developing potential treatments for advanced AD patients. Finally, pharmacological sleep modulators could potentially alter fine-tuned neurochemical brain systems directly (i.e., bypass sleep and their main target) and have unspecific secondary effects confounding the interpretation of results. Therefore, future studies should aim at non-pharmacological sleep modifying methods, such as auditory stimulation of sleep slow oscillations (Dias et al., 2024a; Dias et al., 2024b; Fattinger et al., 2019; Moreira et al., 2021; Ngo et al., 2013; Papalambros et al., 2017; Wunderlin et al., 2023; Zeller et al., 2024), to potentially alter neuropathological hallmarks and consequently delay or reverse AD symptoms.

5 Conclusion

Overall, we show direct and differential associations between SWA increase, plaque deposition, and memory function after prolonged treatment of cohorts at different disease stages, suggesting sleep to be a promising therapeutic target for neuropathology and cognitive impairment in AD. Moreover, our finding that sleep has a restorative effect on cognition after early-onset interventions proposes that identifying individuals at risk for developing AD before significant neuropathological progression is critical to arresting or delaying the onset and/or progression of the disease.

Scope statement

A staggering amount of people worldwide live with AD. Despite extensive efforts from the academy and industry, no cure is available to date. Sleep may be a modifiable factor involved in the onset, progression, and potentially also treatment of AD. However, knowledge regarding important aspects of sleep-targeted treatments is missing, e.g., adequate window of opportunity for their efficacious application, minimal duration, or effect on both pathology and cognition. This manuscript investigates the effect of pharmacologically enhanced sleep depth in amyloid neuropathology and cognition in a mouse model of AD. Our results demonstrated that enhanced sleep depth influenced amyloid pathology in both early- and moderately advanced-stage of the disease; however, cognitive benefits were only present in the early-stage group. This study is highly relevant to the field as it addresses gaps in knowledge regarding the timing, duration, and cognitive effects of sleep interventions in AD treatment. Our study advocates for further mechanistic research and the launch of larger scale preclinical investigations in early AD populations.

Data availability statement

The raw data supporting the conclusions of this article will be made available by the authors, without undue reservation.

Ethics statement

The animal study was approved by the Veterinary Office Canton Zurich. The study was conducted in accordance with the local legislation and institutional requirements.

Author contributions

Funding

Generative AI statement

The authors declare that no Generative AI was used in the creation of this manuscript.

Acknowledgments

Publisher's note

All claims expressed in this article are solely those of the authors and do not necessarily represent those of their affiliated organizations, or those of the publisher, the editors and the reviewers. Any product that may be evaluated in this article, or claim that may be made by its manufacturer, is not guaranteed or endorsed by the publisher.

Conflict of interest

The authors declare that the research was conducted in the absence of any commercial or financial relationships that could be construed as a potential conflict of interest.

References

Aslanyan, V., Ortega, N., Fenton, L., Harrison, T. M., Raman, R., Mack, W. J., et al. (2023). Protective effects of sleep duration and physical activity on cognitive performance are influenced by β-amyloid and brain volume but not tau burden among cognitively unimpaired older adults. *Neuroimage Clin.* 39:103460:103460. doi: 10.1016/j.nicl.2023.103460

Benzing, W. C., Wujek, J. R., Ward, E. K., Shaffer, D., Ashe, K. H., Younkin, S. G., et al. (1999). Evidence for glial-mediated inflammation in aged APP(SW) transgenic mice. *Neurobiol. Aging* 20, 581–589. doi: 10.1016/S0197-4580(99)00065-2

Bero, A. W., Yan, P., Roh, J. H., Cirrito, J. R., Stewart, F. R., Raichle, M. E., et al. (2011). Neuronal activity regulates the regional vulnerability to amyloid-β deposition. *Nat. Neurosci.* 14, 750–756. doi: 10.1038/nn.2801

Bianchetti, A., Scuratti, A., Zanetti, O., Binetti, G., Frisoni, G. B., Magni, E., et al. (1995). Predictors of mortality and institutionalization in Alzheimer disease patients 1 year after discharge from an Alzheimer dementia unit. *Dementia* 6, 108–112. doi: 10.1159/000106930

Braak, H., and Braak, E. (1995). Staging of Alzheimer's disease-related neurofibrillary changes. *Neurobiol. Aging* 16, 271–278. doi: 10.1016/0197-4580(95)00021-6

Branger, P., Arenaza-Urquijo, E. M., Tomadesso, C., Mezenge, F., Andre, C., de Flores, R., et al. (2016). Relationships between sleep quality and brain volume, metabolism, and amyloid deposition in late adulthood. *Neurobiol. Aging* 41, 107–114. doi: 10.1016/j.neurobiolaging.2016.02.009

Brookmeyer, R., Johnson, E., Ziegler-Graham, K., and Arrighi, H. M. (2007). Forecasting the global burden of Alzheimer's disease. *Alzheimers Dement.* 3, 186–191. doi: 10.1016/j.jalz.2007.04.381

Buchele, F., Morawska, M. M., Schreglmann, S. R., Penner, M., Muser, M., Baumann, C. R., et al. (2016). Novel rat model of weight drop-induced closed diffuse traumatic brain injury compatible with electrophysiological recordings of vigilance states. *J. Neurotrauma* 33, 1171–1180. doi: 10.1089/neu.2015.4001

Casali, B. T., and Landreth, G. E. (2016). Aβ extraction from murine brain homogenates. *Bio Protoc* 6:e1787. doi: 10.21769/BioProtoc.1787

Cirrito, J. R., Yamada, K. A., Finn, M. B., Sloviter, R. S., Bales, K. R., May, P. C., et al. (2005). Synaptic activity regulates interstitial fluid amyloid-beta levels in vivo. *Neuron* 48, 913–922. doi: 10.1016/j.neuron.2005.10.028

Deacon, R. M., and Rawlins, J. N. (2006). T-maze alternation in the rodent. *Nat. Protoc.* 1, 7–12. doi: 10.1038/nprot.2006.2

Dias, I., Baumann, C. R., and Noain, D. (2024a). mCLAS adaptively rescues disease-specific sleep and wake phenotypes in neurodegeneration. *Sleep Med.* 124, 704–716. doi: 10.1016/j.sleep.2024.11.009

Dias, I., Kollarik, S., Siegel, M., Baumann, C. R., Moreira, C. G., and Noain, D. (2024b). Novel murine closed-loop auditory stimulation paradigm elicits macrostructural sleep benefits in neurodegeneration. *J. Sleep Res.* e14316. doi: 10.1111/jsr.14316

Fattinger, S., Heinzle, B. B., Ramantani, G., Abela, L., Schmitt, B., and Huber, R. (2019). Closed-loop acoustic stimulation during sleep in children with epilepsy: a hypothesis-driven novel approach to interact with spike-wave activity and pilot data assessing feasibility. *Front. Hum. Neurosci.* 13:166. doi: 10.3389/fnhum.2019.00166

Field, A. (2012) *Discovering statistics using R*. Sage publications ltd.

Hossain, M. F., Uddin, M. S., Uddin, G. M. S., Sumsuzzman, D. M., Islam, M. S., Barreto, G. E., et al. (2019). Melatonin in Alzheimer's disease: a latent endogenous regulator of neurogenesis to mitigate Alzheimer's neuropathology. *Mol. Neurobiol.* 56, 8255–8276. doi: 10.1007/s12035-019-01660-3

Hossain, M. F., Wang, N., Chen, R., Li, S., Roy, J., Uddin, M. G., et al. (2021). Exploring the multifunctional role of melatonin in regulating autophagy and sleep to mitigate Alzheimer's disease neuropathology. *Ageing Res. Rev.* 67:101304. doi: 10.1016/j.arr.2021.101304

Hsiao, K., Chapman, P., Nilsen, S., Eckman, C., Harigaya, Y., Younkin, S., et al. (1996). Correlative memory deficits, Abeta elevation, and amyloid plaques in transgenic mice. *Science* 274, 99–103. doi: 10.1126/science.274.5284.99

Iliff, J. J., Wang, M., Liao, Y., Plogg, B. A., Peng, W., Gundersen, G. A., et al. (2012). A paravascular pathway facilitates CSF flow through the brain parenchyma and the clearance of interstitial solutes, including amyloid β. *Sci. Transl. Med.* 4:147ra111. doi: 10.1126/scitranslmed.3003748

Ishii, M., Wang, G., Racchumi, G., Dyke, J. P., and Iadecola, C. (2014). Transgenic mice overexpressing amyloid precursor protein exhibit early metabolic deficits and a pathologically low leptin state associated with hypothalamic dysfunction in arcuate neuropeptide Y neurons. *J. Neurosci.* 34, 9096–9106. doi: 10.1523/JNEUROSCI.0872-14.2014

Jagirdar, R., Fu, C. H., Park, J., Corbett, B. F., Seibt, F. M., Beierlein, M., et al. (2021). Restoring activity in the thalamic reticular nucleus improves sleep architecture and reduces Aβ accumulation in mice. *Sci. Transl. Med.* 13:eabh4284. doi: 10.1126/scitranslmed.abh4284

Ju, Y. E., McLeland, J. S., Toedebusch, C. D., Xiong, C., Fagan, A. M., Duntley, S. P., et al. (2013). Sleep quality and preclinical Alzheimer disease. *JAMA Neurol.* 70, 587–593. doi: 10.1001/jamaneurol.2013.2334

Ju, Y. E., Lucey, B. P., and Holtzman, D. M. (2014). Sleep and Alzheimer disease pathology—a bidirectional relationship. *Nat. Rev. Neurol.* 10, 115–119. doi: 10.1038/nrneurol.2013.269

Kang, J. E., Lim, M. M., Bateman, R. J., Lee, J. J., Smyth, L. P., Cirrito, J. R., et al. (2009). Amyloid-beta dynamics are regulated by orexin and the sleep-wake cycle. *Science* 326, 1005–1007. doi: 10.1126/science.1180962

Kaprio, J., and Koskenvuo, M. (2002). Genetic and environmental factors in complex diseases: the older Finnish twin cohort. *Twin Res.* 5, 358–365. doi: 10.1375/136905202320906093

Kawarabayashi, T., Younkin, L. H., Saido, T. C., Shoji, M., Ashe, K. H., and Younkin, S. G. (2001). Age-dependent changes in brain, CSF, and plasma amyloid (beta) protein in the Tg2576 transgenic mouse model of Alzheimer's disease. *J. Neurosci.* 21, 372–381. doi: 10.1523/JNEUROSCI.21-02-00372.2001

Kim, J., Onstead, L., Randle, S., Price, R., Smithson, L., Zwizinski, C., et al. (2007). Abeta40 inhibits amyloid deposition in vivo. *J. Neurosci.* 27, 627–633. doi: 10.1523/JNEUROSCI.4849-06.2007

Klein, C., Mathis, C., Leva, G., Patte-Mensah, C., Cassel, J. C., Maitre, M., et al. (2015). γ-Hydroxybutyrate (xyrem) ameliorates clinical symptoms and neuropathology in a mouse model of Alzheimer's disease. *Neurobiol. Aging* 36, 832–844. doi: 10.1016/j.neurobiolaging.2014.10.003

Knopman, D. S., Jones, D. T., and Greicius, M. D. (2019). Failure to demonstrate efficacy of aducanumab: an analysis of the EMERGE and ENGAGE trials as reported by biogen. *Alzheimers Dement.* 17, 696–701. doi: 10.1002/alz.12213

Kollarik, S., Dias, I., Moreira, C. G., Bimbiryte, D., Miladinovic, D., Buhmann, J. M., et al. (2023). Natural age-related slow-wave sleep alterations onset prematurely in the Tg2576 mouse model of Alzheimer's disease. *Neurodegener Dis* 22, 55–67. doi: 10.1159/000527786

Lee, Y. F., Gerashchenko, D., Timofeev, I., Bacskai, B. J., and Kastanenka, K. V. (2020). Slow wave sleep is a promising intervention target for Alzheimer's disease. *Front. Neurosci.* 14:705. doi: 10.3389/fnins.2020.00705

Lim, A. S., Kowgier, M., Yu, L., Buchman, A. S., and Bennett, D. A. (2013). Sleep fragmentation and the risk of incident Alzheimer's disease and cognitive decline in older persons. *Sleep* 36, 1027–1032. doi: 10.5665/sleep.2802

Lin, L., Huang, Q. X., Yang, S. S., Chu, J., Wang, J. Z., and Tian, Q. (2013). Melatonin in Alzheimer's disease. *Int. J. Mol. Sci.* 14, 14575–14593. doi: 10.3390/ijms140714575

Ling, Z. Q., Tian, Q., Wang, L., Fu, Z. Q., Wang, X. C., Wang, Q., et al. (2009). Constant illumination induces Alzheimer-like damages with endoplasmic reticulum involvement and the protection of melatonin. *J. Alzheimers Dis.* 16, 287–300. doi: 10.3233/JAD-2009-0949

Livingston, G., Huntley, J., Liu, K. Y., Costafreda, S. G., Selbaek, G., Alladi, S., et al. (2024). Dementia prevention, intervention, and care: 2024 report of the lancet standing commission. *Lancet* 404, 572–628. doi: 10.1016/S0140-6736(24)01296-0

Lucey, B. P., Wisch, J., Boerwinkle, A. H., Landsness, E. C., Toedebusch, C. D., McLeland, J. S., et al. (2021). Sleep and longitudinal cognitive performance in preclinical and early symptomatic Alzheimer's disease. *Brain* 144, 2852–2862. doi: 10.1093/brain/awab272

Mander, B. A., Marks, S. M., Vogel, J. W., Rao, V., Lu, B., Saletin, J. M., et al. (2015). β-Amyloid disrupts human NREM slow waves and related hippocampus-dependent memory consolidation. *Nat. Neurosci.* 18, 1051–1057. doi: 10.1038/nn.4035

Mander, B. A., Winer, J. R., and Walker, M. P. (2017). Sleep and Human Aging. *Neuron* 94, 19–36. doi: 10.1016/j.neuron.2017.02.004

Mendelsohn, A. R., and Larrick, J. W. (2013). Sleep facilitates clearance of metabolites from the brain: glymphatic function in aging and neurodegenerative diseases. *Rejuvenation Res.* 16, 518–523. doi: 10.1089/rej.2013.1530

Miladinović, Đ., Muheim, C., Bauer, S., Spinnler, A., Noain, D., Bandarabadi, M., et al. (2019). SPINDLE: end-to-end learning from EEG/EMG to extrapolate animal sleep scoring across experimental settings, labs and species. *PLoS Comput. Biol.* 15:e1006968:e1006968. doi: 10.1371/journal.pcbi.1006968

Morawska, M. M., Moreira, C. G., Ginde, V. R., Valko, P. O., Weiss, T., Buchele, F., et al. (2021). Slow-wave sleep affects synucleinopathy and regulates proteostatic processes in mouse models of Parkinson's disease. *Sci. Transl. Med.* 13:eabe7099. doi: 10.1126/scitranslmed.abe7099

Moreira, C. G., Baumann, C. R., Scandella, M., Nemirovsky, S. I., Leach, S., Huber, R., et al. (2021). Closed-loop auditory stimulation method to modulate sleep slow waves and motor learning performance in rats. *eLife* 10:e68043. doi: 10.7554/eLife.68043

Musiek, E. S., and Holtzman, D. M. (2016). Mechanisms linking circadian clocks, sleep, and neurodegeneration. *Science* 354, 1004–1008. doi: 10.1126/science.aah4968

Ngo, H. V., Martinetz, T., Born, J., and Mölle, M. (2013). Auditory closed-loop stimulation of the sleep slow oscillation enhances memory. *Neuron* 78, 545–553. doi: 10.1016/j.neuron.2013.03.006

Nguyen Ho, P. T., Hoepel, S. J. W., Rodriguez-Ayllon, M., Luik, A. I., Vernooij, M. W., and Neitzel, J. (2024). Sleep, 24-hour activity rhythms, and subsequent amyloid-beta pathology. *JAMA Neurol.* 81:824. doi: 10.1001/jamaneurol.2024.1755

Nitsch, R. M., Farber, S. A., Growdon, J. H., and Wurtman, R. J. (1993). Release of amyloid beta-protein precursor derivatives by electrical depolarization of rat hippocampal slices. *Proc. Natl. Acad. Sci. USA* 90, 5191–5193. doi: 10.1073/pnas.90.11.5191

Niu, L., Zhang, F., Xu, X., Yang, Y., Li, S., Liu, H., et al. (2022). Chronic sleep deprivation altered the expression of circadian clock genes and aggravated Alzheimer's disease neuropathology. *Brain Pathol.* 32:e13028. doi: 10.1111/bpa.13028

Ooms, S., Overeem, S., Besse, K., Rikkert, M. O., Verbeek, M., and Claassen, J. A. (2014). Effect of 1 night of total sleep deprivation on cerebrospinal fluid beta-amyloid 42 in healthy middle-aged men: a randomized clinical trial. *JAMA Neurol.* 71, 971–977. doi: 10.1001/jamaneurol.2014.1173

Papalambros, N. A., Santostasi, G., Malkani, R. G., Braun, R., Weintraub, S., Paller, K. A., et al. (2017). Acoustic enhancement of sleep slow oscillations and concomitant memory improvement in older adults. *Front. Hum. Neurosci.* 11:109. doi: 10.3389/fnhum.2017.00109

Park, J., Kim, D. Y., Hwang, G. S., and Han, I. O. (2023). Repeated sleep deprivation decreases the flux into hexosamine biosynthetic pathway/O-GlcNAc cycling and aggravates Alzheimer's disease neuropathology in adult zebrafish. *J. Neuroinflammation* 20:257. doi: 10.1186/s12974-023-02944-1

Passeri, E., Elkhoury, K., Morsink, M., Broersen, K., Linder, M., Tamayol, A., et al. (2022). Alzheimer's disease: treatment strategies and their limitations. *Int. J. Mol. Sci.* 23:13954. doi: 10.3390/ijms232213954

Robinson, D. M., and Keating, G. M. (2007). Sodium oxybate. *CNS Drugs* 21, 337–354. doi: 10.2165/00023210-200721040-00007

Roh, J. H., Huang, Y., Bero, A. W., Kasten, T., Stewart, F. R., Bateman, R. J., et al. (2012). Disruption of the sleep-wake cycle and diurnal fluctuation of beta-amyloid in mice with Alzheimer's disease pathology. *Sci. Transl. Med.* 4:150ra122. doi: 10.1126/scitranslmed.3004291

Sperling, R. A., Aisen, P. S., Beckett, L. A., Bennett, D. A., Craft, S., Fagan, A. M., et al. (2011). Toward defining the preclinical stages of Alzheimer's disease: recommendations from the National Institute on Aging-Alzheimer's Association workgroups on diagnostic guidelines for Alzheimer's disease. *Alzheimers Dement.* 7, 280–292. doi: 10.1016/j.jalz.2011.03.003

Spira, A. P., Gamaldo, A. A., An, Y., Wu, M. N., Simonsick, E. M., Bilgel, M., et al. (2013). Self-reported sleep and β-amyloid deposition in community-dwelling older adults. *JAMA Neurol.* 70, 1537–1543. doi: 10.1001/jamaneurol.2013.4258

Spira, A. P., An, Y., Wu, M. N., Owusu, J. T., Simonsick, E. M., Bilgel, M., et al. (2018). Excessive daytime sleepiness and napping in cognitively normal adults: associations with subsequent amyloid deposition measured by PiB PET. *Sleep* 41. doi: 10.1093/sleep/zsy152

Sprecher, K. E., Bendlin, B. B., Racine, A. M., Okonkwo, O. C., Christian, B. T., Koscik, R. L., et al. (2015). Amyloid burden is associated with self-reported sleep in nondemented late middle-aged adults. *Neurobiol. Aging* 36, 2568–2576. doi: 10.1016/j.neurobiolaging.2015.05.004

Tampi, R. R., Forester, B. P., and Agronin, M. (2021). Aducanumab: evidence from clinical trial data and controversies. *Drugs Context* 10, 1–9. doi: 10.7573/dic.2021-7-3

Vicente De Carvalho, J. S., Oliveira, I., Rosa, R., Barata, C., Fradinho, M., Oliveira, L., et al. (2018). Sleep quality and quality of life in physicians and nurses working at a central hospital. *Eur. Respir. J.* 52:PA4372. doi: 10.1183/13993003.congress-2018.PA4372

Virta, J. J., Heikkila, K., Perola, M., Koskenvuo, M., Raiha, I., Rinne, J. O., et al. (2013). Midlife sleep characteristics associated with late life cognitive function. *Sleep* 36:1533-41, 1541A. doi: 10.5665/sleep.3052

Wang, C., and Holtzman, D. M. (2020). Bidirectional relationship between sleep and Alzheimer's disease: role of amyloid, tau, and other factors. *Neuropsychopharmacology* 45, 104–120. doi: 10.1038/s41386-019-0478-5

Wennberg, A. M. V., Wu, M. N., Rosenberg, P. B., and Spira, A. P. (2017). Sleep disturbance, cognitive decline, and dementia: a review. *Semin. Neurol.* 37, 395–406. doi: 10.1055/s-0037-1604351

Westerman, M. A., Cooper-Blacketer, D., Mariash, A., Kotilinek, L., Kawarabayashi, T., Younkin, L. H., et al. (2002). The relationship between Abeta and memory in the Tg2576 mouse model of Alzheimer's disease. *J. Neurosci.* 22, 1858–1867. doi: 10.1523/JNEUROSCI.22-05-01858.2002

Wilckens, K. A., Hall, M. H., Nebes, R. D., Monk, T. H., and Buysse, D. J. (2016). Changes in cognitive performance are associated with changes in sleep in older adults with insomnia. *Behav. Sleep Med.* 14, 295–310. doi: 10.1080/15402002.2014.1002034

Wilcock, D. M., Gordon, M. N., and Morgan, D. (2006). Quantification of cerebral amyloid angiopathy and parenchymal amyloid plaques with Congo red histochemical stain. *Nat. Protoc.* 1, 1591–1595. doi: 10.1038/nprot.2006.277

Wiltfang, J., Esselmann, H., Bibl, M., Hull, M., Hampel, H., Kessler, H., et al. (2007). Amyloid β peptide ratio 42/40 but not Aβ42 correlates with phospho-tau in patients with low- and high-CSF Aβ40 load. *J. Neurochem.* 101, 1053–1059. doi: 10.1111/j.1471-4159.2006.04404.x

Wunderlin, M., Zeller, C. J., Senti, S. R., Feher, K. D., Suppiger, D., Wyss, P., et al. (2023). Acoustic stimulation during sleep predicts long-lasting increases in memory performance and beneficial amyloid response in older adults. *Age Ageing* 52:13954. doi: 10.1093/ageing/afad228

Zeller, C. J., Wunderlin, M., Wicki, K., Teunissen, C. E., Nissen, C., Zust, M. A., et al. (2024). Multi-night acoustic stimulation is associated with better sleep, amyloid dynamics, and memory in older adults with cognitive impairment. *Geroscience* 46, 6157–6172. doi: 10.1007/s11357-024-01195-z

Zhao, Q., Maci, M., Miller, M. R., Zhou, H., Zhang, F., Algamal, M., et al. (2023). Sleep restoration by optogenetic targeting of GABAergic neurons reprograms microglia and ameliorates pathological phenotypes in an Alzheimer's disease model. *Mol. Neurodegener.* 18:93. doi: 10.1186/s13024-023-00682-9

Zoltowska, K. M., Maesako, M., and Berezovska, O. (2016). Interrelationship between changes in the amyloid β 42/40 ratio and presenilin 1 conformation. *Mol. Med.* 22, 329–337. doi: 10.2119/molmed.2016.00127